Journal of Structural Geology, Vol. 5, No. 3/4, pp. 411 to 418, 1983
Printed in Great Britain

0191-8141/83 $3.00 + 0.00

Strain pattern in the Aar Granite (Central Alps): orthogneiss developed by bulk inhomogeneous flattening

PIERRE CHOUKROUNE and DENIS GAPAIS

Centre Armoricain d'Etude Structurale des Socles (CNRS),
Université de Rennes, 35042 Rennes Cédex, France

(*Received 7 July* 1982; *accepted in revised form* 15 *December* 1982)

Abstract—The central part of the Aar Granite (Aar Valley) shows lens-shaped domains of low strain separated by anastomosing domains of high strain. A comparable pattern is found on all scales of observation. Deformation gradients are outlined by a gradual change from isotropic granite to orthogneiss and locally ultramylonites. Ultramylonites are concentrated within conjugate ductile shear zones. Where moderate, the strain is concentrated in very narrow small-scale faults which affect relatively undeformed granite. Within foliated domains, finite strain measurements on deformed xenoliths indicate that (i) strain intensity increases gradually with grain size reduction and (ii) finite-strain ellipsoids are of flattening type irrespective of the degree of mylonitization. The pattern of small-scale faulting, the trends of the regional foliation and the orientation of ductile shear zones are consistent with a bulk strain field of flattening type throughout progressive deformation.

INTRODUCTION AND GEOLOGICAL SETTING

THE AAR Massif, situated in Central Switzerland (Central Alps), belongs to the Infrahelvetic complex where it forms the basement of Helvetic nappes (Fig. 1). It is mainly made of high-grade metamorphic rocks (gneisses and amphibolites) which are intruded by granitic rocks of Hercynian age (Steck 1966, 1968).

This paper describes the ductile deformation of these granitic rocks of the central part of the massif, in the region of the Aar Valley (Fig. 1). These rocks have been deformed during the Alpine orogeny under greenschist-facies metamorphic conditions (Steck 1968, Voll 1976). In fact, all deformation structures which have been recognized in the granite have been shown to be of Alpine age (Steck 1966, 1968, Steck *et al.* 1979). Indeed, the only regional penetrative foliation which affects the granite passes into the overlying Helvetic units (Milnes & Pfiffner 1977). Steck (1968) gave a detailed description of all structures in the granite in terms of superposed deformation phases. The main sets of these structures are reconsidered here and are shown to outline a consistent general strain pattern.

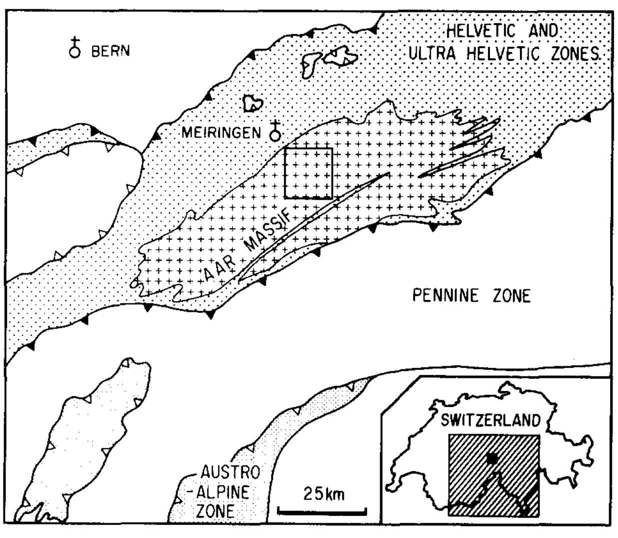

Fig. 1. Simplified tectonic map of the Central Alps and its geographical locality (inset). The area studied is outlined on the Aar Massif.

Along the Aar Valley, large volumes of granite with no fabric (isotropic) or a weak grain-shape fabric are preserved. Furthermore, a gradual change from isotropic granite to orthogneiss is observed on different scales. The nature of the structures and their associated strain patterns should provide constraints for a model of progressive deformation. Such models are necessary if the behaviour of the continental crust during orogenic processes is to be discussed. Further information could be gained through comparisons with granitic rocks deformed in other tectonic environments, such as syntectonic granites affected by shear deformation (Berthé *et al.* 1979, Iglesias & Choukroune 1980).

First, we describe the general geometry of structures (foliation, deformation zones) on the map and outcrop scales. Then, macroscopic characteristics of deformation gradients and associated increasing degree of mylonitization will be described and compared with local finite-strain analyses. General aspects of strain patterns will be discussed in terms of progressive deformation and will be used as a basis to propose a geometric and kinematic deformation model of the granite in the area. Results will be compared with examples of orthogneiss development in other areas.

GEOMETRY OF LARGE-SCALE STRUCTURES

The granite studied shows a regional foliation defined by the preferred orientation of grain shapes. An associated mineral stretching lineation is present but is generally only weakly developed. The foliation strikes consistently ENE–WSW and dips steeply towards the south (typically around 70°). The lineation lies close to the dip of the foliation plane. The foliation and lineation have been used as the principal strain plane *XY* and the principal stretching direction *X*, respectively.

Mapping of structures reveals a very heterogeneous strain pattern (Fig. 2). The degree of development of the foliation varies strongly and the granite appears locally rather isotropic and undeformed. Non-foliated to weakly-foliated zones appear typically as three-dimensional lens-shaped pods surrounded by foliated material (Fig. 2). These lenses are oriented parallel to the regional foliation.

Ductile shear zones within the granite are revealed by the occurrence of granite mylonites and ultramylonites, and are marked by local variations of foliation trajectories (Fig. 2). Such zones of large strain occur on different scales. They are often found along margins of weakly deformed lenses but also away from lenses, within the regionally foliated material. The direction and sense of shear depends upon the orientation of the shear zones with respect to the regional foliation. Dextral and sinistral strike-slip type shear zones, trending WNW–ESE and NE–SW, respectively, are observed. They are steeply dipping and conjugate relative to the foliation (Fig. 2a). Reverse shear zones are also well developed (Fig. 2b). They dip generally southwards and trend ENE–WSW, close to the trend of the regional foliation. At map scale, the set of dextral strike-slip shear zones is better developed than the conjugate sinistral one (Fig. 2a) (see Steck 1968).

ASPECTS OF INHOMOGENEOUS STRAIN AROUND WEAKLY-DEFORMED LENSES

Lens-shaped patterns of the type described above occur on all scales. Examples are shown in Fig. 3. Structural mapping around an outcrop-scale lens has allowed us to define the geometry of structures associated with the change from initial isotropic granite to orthogneiss (Fig. 4).

Within the lens, deformation is mainly concentrated along sets of faults. These are very narrow ductile faults (typically less than 1 cm wide). They mimic the orientation of the margin of the lens and define it locally. Fault planes commonly show striations which allow the direction and the sense of displacement to be determined. The observed geometry of major sets of faults (Fig. 4) is consistent with that of ductile shear zones seen on a large scale (Fig. 2). Various combinations between purely strike-slip faults and purely reverse faults occur as a function of their orientation with respect to the regional foliation and the long axis of the lens (Fig. 4, stereonet). Arrays of small-scale faults have the same geometry over the whole area studied (Fig. 5a).

This strongly discontinuous deformation (which is non-penetrative on a sample scale) is best developed at the margins of outcrop-scale lenses. It divides the rock into rhomb-shaped domains whose long axes parallel the regional foliation, as described by Mitra (1979), and appears as the transition between isotropic granite and penetratively foliated granite. A compatible relationship is found between bulk displacement patterns along faults and the orientation of the bulk strain field associated with the regional penetrative deformation (Fig. 5). This is

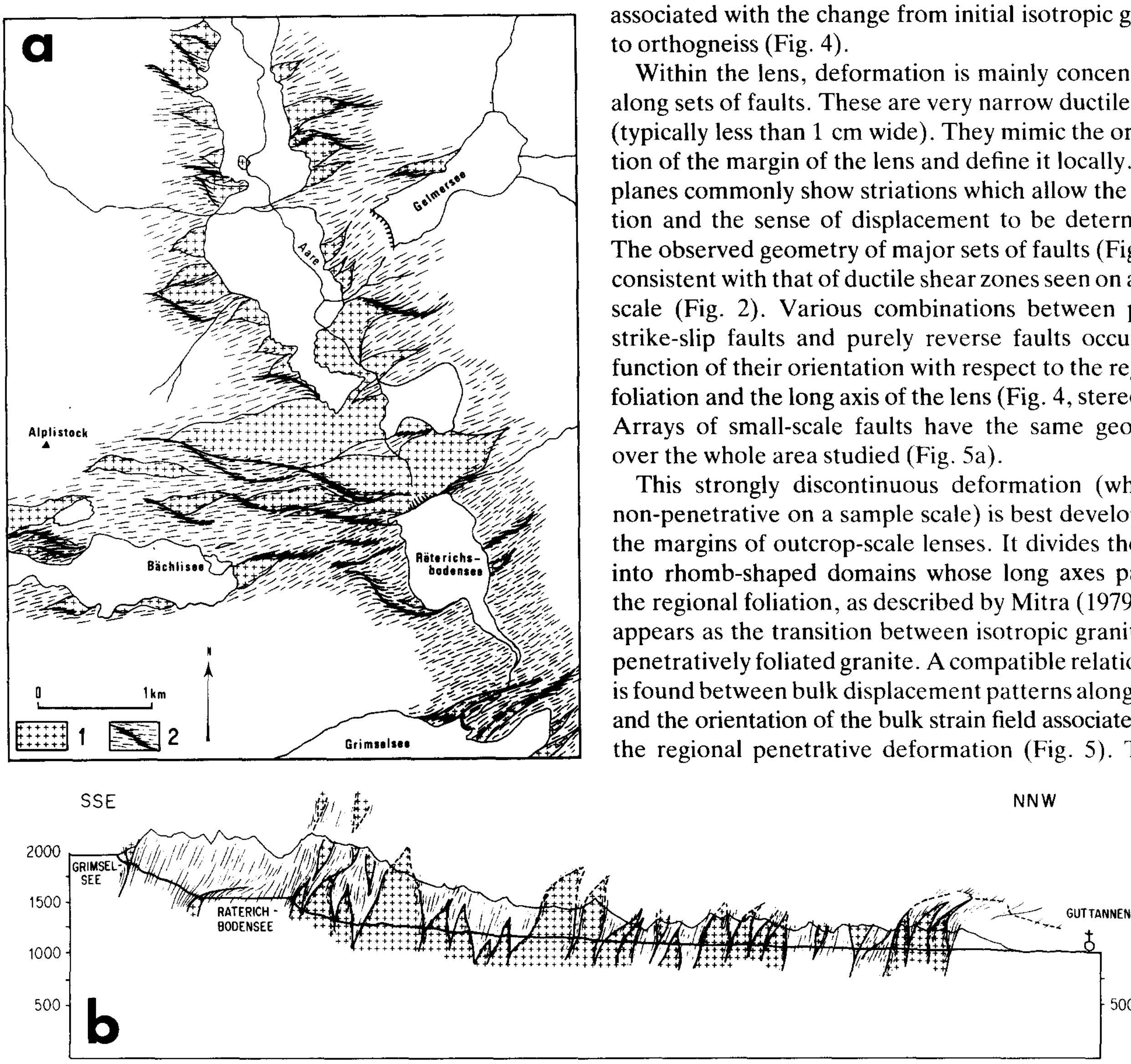

Fig. 2. Aspects of foliation trajectories. The regional stretching is subvertical. (a) Map of the region of the Aar Valley (see Fig. 1); 1, isotropic or weakly foliated granite; 2, trace of regional foliation and of major deformation zones within foliated granite; in blank, areas not exposed or not mapped. (b) Vertical cross-section along the Aar Valley; symbols and scale as in (a).

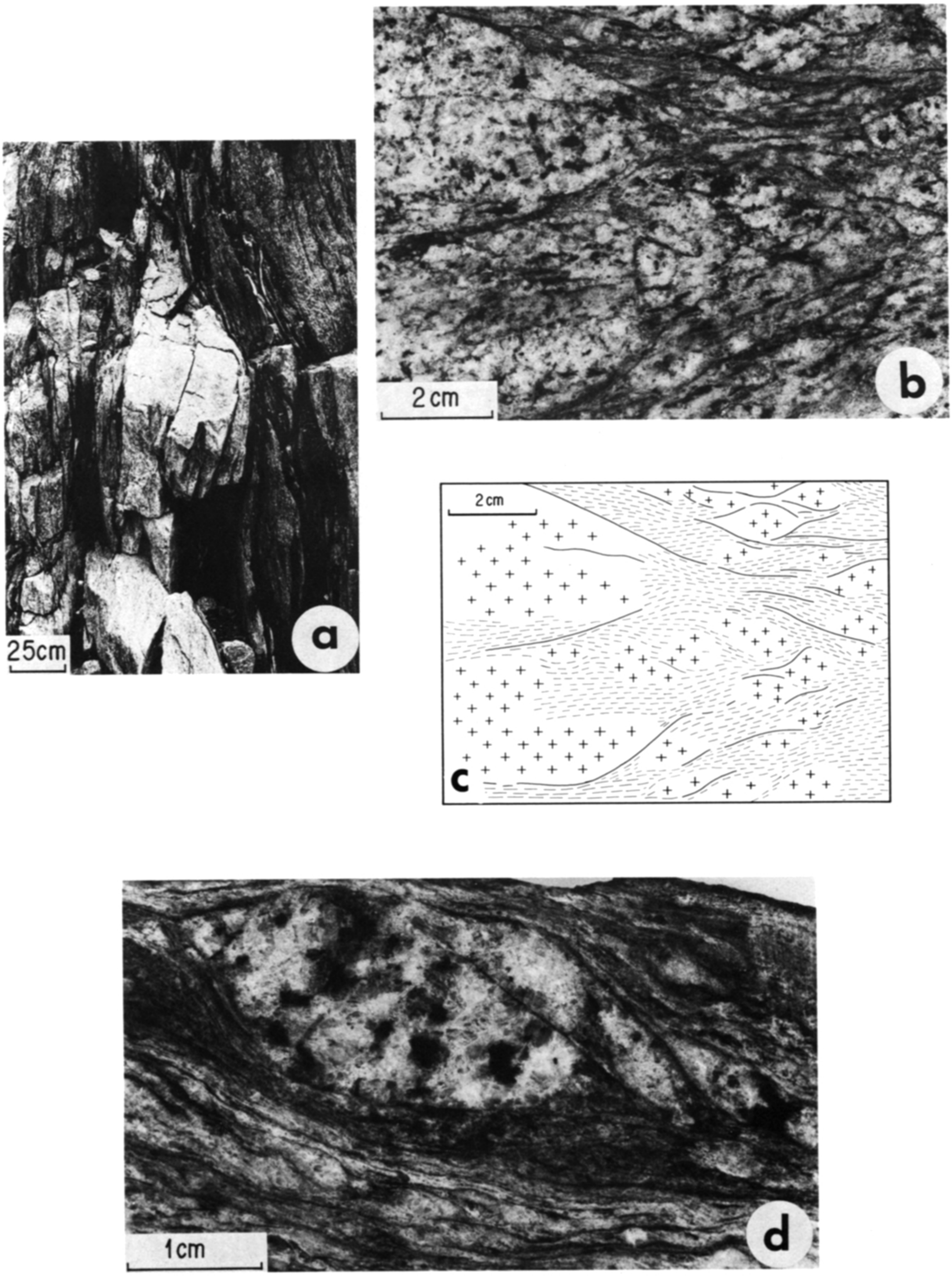

Fig. 3. Aspects of heteregeneous strain at the outcrop and sample scales. Lens-shaped pods of weakly deformed granite are surrounded by foliated material. (c) is a sketch of (b).

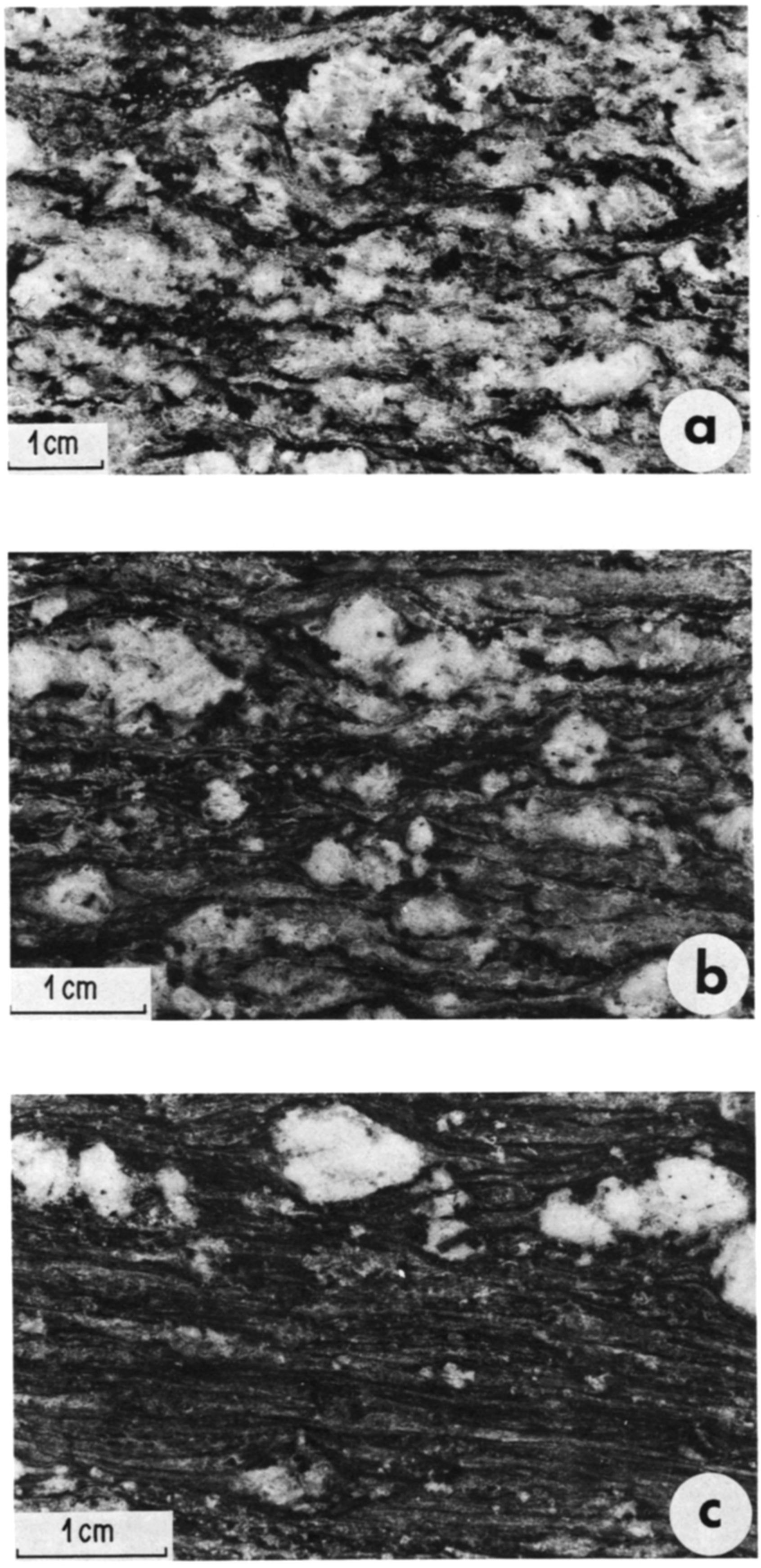

Fig. 6. Successive stages of increasing penetrative deformation of initially isotropic Aar Granite.

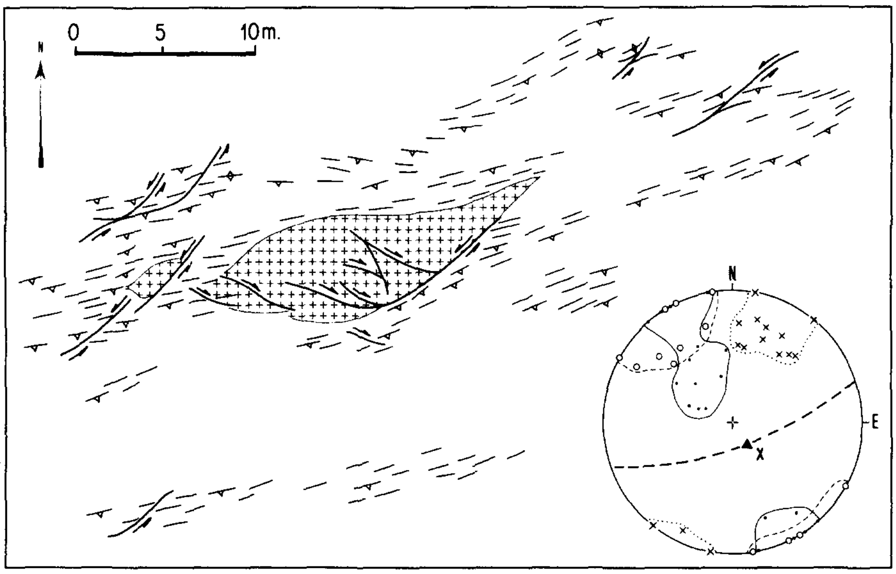

Fig. 4. Structural map of an outcrop-scale pod of weakly deformed granite. Trends of regional foliation and of small-scale faults are shown. Stereographic projection (lower hemisphere) shows the distribution of poles to fault planes. Crosses, dextral faults; open circles, sinistral faults; dots, thrust and vertical faults. Average orientations of regional foliation (dashed arc) and stretching lineation X are shown on the diagram.

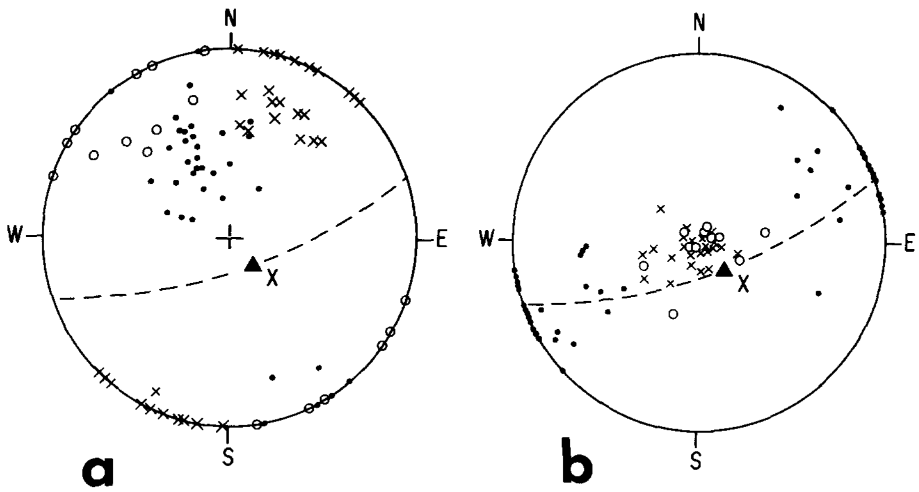

Fig. 5. Geometry of fault array in the area studied: (a) poles to fault planes; (b) poles to planes of motion along faults; see text for explanations. Symbols as for Fig. 4.

underlined by the good agreement which is found between regional strain axes (those given by penetrative foliation and lineation) and the distribution of poles to planes of motion along faults. (The plane of motion along a fault is defined as the plane which is perpendicular to the fault plane and contains the striations; Arthaud 1969 and Fig. 5b.)

In general, perturbations of the foliation in the vicinity of lenses are minor (Figs. 2 and 4). Foliation trajectories have a rather constant orientation and outline a symmetrical pattern around lenses (Figs. 4 and 3b & c). At a sample scale, this pattern can often be related to a gradual change from isotropic granite to orthogneiss across the boundary of lenses. That is, refractions are weak across poorly defined interfaces, marked by small, progressive changes in the degree of penetrative deformation (Figs. 3b & c). In contrast, strong refractions of the foliation occur locally across sharp interfaces where the amount of deformation varies abruptly (e.g. the interface between isotropic material and ultramylonites of Fig. 3d). This will be discussed in following sections.

DUCTILE-DEFORMATION GRADIENTS

Starting from isotropic material, three general stages of increasing penetrative deformation can be distinguished in the field (Fig. 6). A marked softening and a decrease in viscosity accompanies the associated grain size reduction, as outlined by foliation refractions (Fig. 3).

Variations in the degree of penetrative deformation are not restricted to local shear zones but also occur within regularly foliated domains on the scale of the regional foliation. That is, the amount of grain-scale deformation may vary without marked changes in the orientation of the resulting foliation and this occurs on different scales. Hence, the regional deformation appears to increase when moving southwards along the Aar Valley. The southern part of the area is more strongly strained, as shown by (i) an increase of the average degree of development of the foliation, (ii) an increase in the amount of foliated material with respect to the isotropic granite and (iii) an increase of the ellipticity of weakly deformed lenses (Fig. 2a).

FINITE STRAIN VERSUS DEGREE OF MYLONITIZATION

Deformed xenoliths have been used for local estimates of the finite-strain ellipsoid. The xenoliths are fine-grained inclusions of magmatic material of relatively basic composition. Measurements relate to zones showing different amounts of grain-scale deformation, up to mylonitized granites, and all relate to regionally foliated material.

Strain measurements have been made at outcrops, within principal planes. For each principal section, the mean axial ratio of xenoliths was obtained from a plot of the length of long axes as a function of the length of short axes, using the least-squares method (Ramsay 1967, p. 193). This method has been found sufficiently accurate because (i) each plot showed a good alignment of points along a straight line passing through the origin, and (ii) the orientation of xenoliths within a given section was approximately constant and parallel to the lineation and/or the trace of the foliation. Also, the lack of significant refraction of the foliation across xenoliths attests to a low viscosity contrast between markers and matrix, and this argues for relatively good estimates of strain.

Results are presented on a Flinn diagram (Fig. 7). They indicate that strain intensity may be very high within fine-grained mylonites (X/Z up to 25) and that a large range of strain intensities is observed. This agrees with the heterogeneity of strain indicated by the foliation refraction across lens margins (Fig. 3).

Measured finite strain ellipsoids are all of the flattening type ($k \leq 0.5$), irrespective of the degree of mylonitization. This is consistent with the planar fabric (weak mineral lineation and strong foliation) which is observed in the rocks. Comparable strain values have also been reported by Steck (1968) in other parts of the massif.

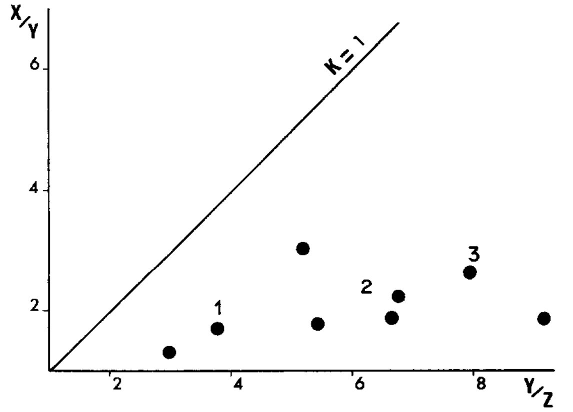

Fig. 7. Flinn diagram showing finite-strain ellipsoids for successive stages of increasing regional penetrative deformation. 1, 2, 3 can be related to Figs. 6 (a), (b) and (c), respectively.

DISCUSSION AND DEFORMATION MODEL

Constraints for a model

Results presented above introduce several constraints on the deformation history which may have led to the observed strain pattern.

Heterogeneity of strain exists on all scales. It is marked by the occurrence of lenticular relics of weakly deformed material which preserve features related to the onset of the deformation. A large part of the bulk strain has accumulated within surrounding foliated domains where the regional foliation has a relatively constant orientation irrespective of the local amount of associated strain. Geometric analogies can be found with P-type band-like structures, as defined by Cobbold (1977); that is, deformation bands mainly associated with differential shortening normal to the bands. In addition, large strains are locally achieved within shear zones where granite ultramylonites have developed. These are typical S-type bands (Cobbold 1977) where deformation is mainly achieved through differential shearing.

It has been shown that there is only one regional foliation. However, structures related to both continuous (penetrative) and discontinuous (non-penetrative) deformation can be developed within a single bulk strain field, and therefore interpreted in terms of one progressive deformation event.

Fabrics and measured finite strain ellipsoids within regionally foliated material show strains of the flattening type with a subvertical direction of principal extension. This, combined with the geometry of structures and deformation gradients, suggests that subhorizontal shortening is a major component of the bulk progressive deformation in the area. The shortening on the bulk scale is partly accommodated through strongly non-coaxial deformation, within non-penetrative ductile fault zones.

Details of physical processes and associated deformation mechanisms on a grain-scale are outside the scope of the present paper. Briefly, the reduction of grain size with increasing deformation is seen to result from combined brittle and ductile processes, according to the considered mineral. It is enhanced by mineralogical transformations such as decay of feldspars; this probably controls the onset and evolution of soft zones as deformation proceeds (Mitra 1978). Other textural evidence (e.g. migration of the quartz phase) indicates important activity of water-enhanced diffusion processes which is likely to favour the production of very heterogeneous states of strain within basement rocks. Also, it may favour the development of P-type deformation bands (Cobbold 1977). Such mineralogical changes are the subject of current research of D.G.

Model of progressive deformation

The model proposed (Fig. 8) is that of a progressive deformation by dominantly bulk heterogeneous flatten-

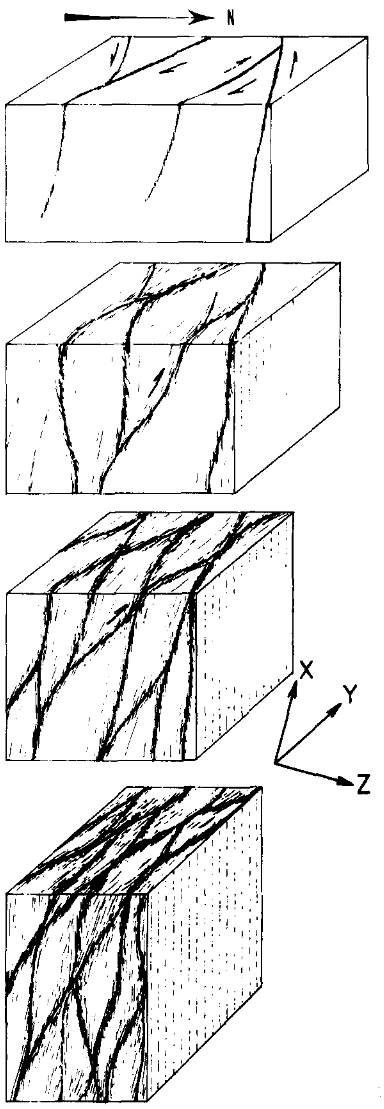

Fig. 8. Four schematic successive stages of bulk progressive deformation of the Aar Granite with respect to strain axes *X*, *Y* and *Z*.

ing within the granitic basement rocks of the Aar Valley.

In this model, deformation proceeds through the combined evolution of anastomosing soft bands of dominantly differential shortening or of differential shearing. Very large finite strains are achieved locally in the latter. The geometry of the resulting patterns of heterogeneous strain is comparable on all scales. Preserved domains of isotropic material are progressively destroyed as deformation proceeds. This results from the development of arrays of narrow, small-scale soft zones through combined chemical and mechanical processes.

Within the *YZ* strain plane (approximately the map plane), the general geometry on all scales argues against a dominantly non-coaxial bulk deformation, although some asymmetry of conjugate strike-slip shear zones is observed (Fig. 2a).

The kinematic interpretation of strain patterns within the *XZ* strain plane (approximately the NNW–SSE vertical plane) is strongly linked to the scale at which structures are observed. Evidence for a large-scale component of thrusting towards the NNW exists within the basement rocks in this part of the Alps (Milnes & Pfiffner 1977, Menard 1980). Indeed, NNW thrusting is clearly observed at boundaries of the Aar Massif (Fig. 2b; Steck 1968). Within the central part of the Aar Valley, the occurrence of dominantly southwards dipping reverse faults also appears to argue for this. However, the symmetrical pattern of weakly deformed lenses and the local constant attitudes of foliation trajectories across strain gradients indicate that the non-coaxial component of the bulk deformation is locally minor at the outcrop-scale.

The general strain pattern in the Aar Granite reveals a bulk shortening type of deformation history whose kinematic characters depend on the local deformation history and on the scale of observations. In fact, most of the observed geometrical features are comparable with those one may expect to result from a bulk heterogeneous coaxial shortening deformation (Bell 1981). Thus, compared with other examples of deformed granites, the model proposed here may be used to describe a natural process of orthogneiss development by bulk coaxial shortening (Fig. 9). In such a deformation history, relative contributions of conjugate shear components to the bulk deformation would be equal, whereas only one major set of shear zones develops during a bulk simple shearing type of deformation history such as in the South Armorican granites (Berthé *et al.* 1979).

CONCLUSIONS

The interpretation of strain patterns in the Aar Granite has led to a geometric and kinematic model of orthogneiss development by bulk heterogeneous shortening of initial isotropic granitic basement. The progressive deformation results in a regional foliation and in strain concentration within arrays of ductile faults. These appear typical of many areas of reworked crystalline basement rocks (Mitra 1979, Ramsay & Allison 1979). The general strain pattern is comparable on all scales and relates to major characteristics of progressive deformation in a relatively simple way.

Structures within the Aar Granite have been shown to result from a single major deformation event. Data presented here emphasize that important crustal thickening associated with subvertical extension occurred within the basement of this part of the Alps (also inferred further east by Milnes & Pfiffner 1977). This is not clearly revealed by observation of upper low-grade units (e.g. Helvetic nappes) where only effects of overthrusting are seen.

Granitic rocks represent large volumes of initially quasi-isotopic and homogeneous crustal material with a simple mineralogy. Aspects of their progressive deformation can often be determined through the analysis of deformation zones where various stages from undeformed to strongly deformed material are present. These render granites of great interest for studying kinematic and mechanical aspects of the deformation of the deep continental crust.

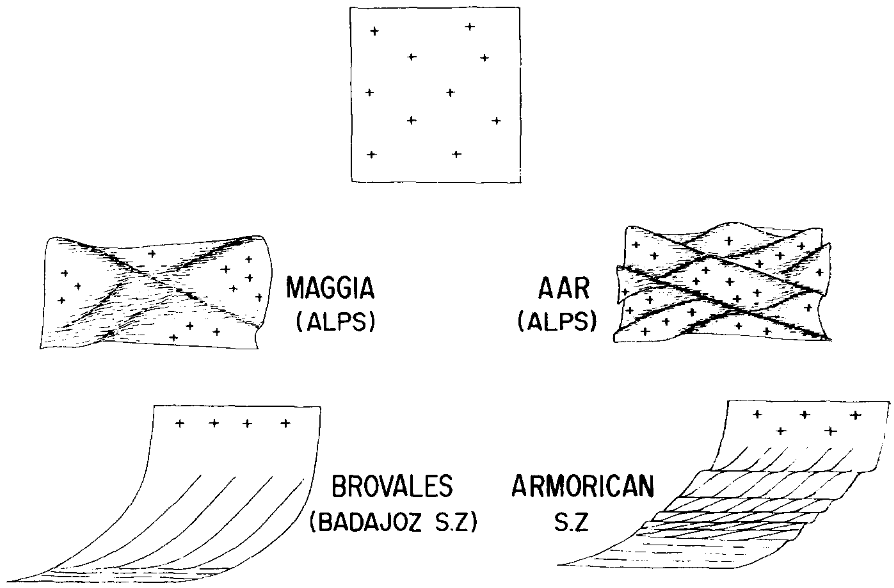

Fig. 9. Sketch of some major types of natural strain patterns as found in initially isotopic granitic rocks showing large strains, according to both kinematic and thermo-mechanical aspects of the progressive deformation. Strain patterns relate to different scales within the massifs. Interpreted from Ramsay & Allison (1979) from the Maggia reworked granitic basement (Alps), Brun & Pons (1981) and Pons (1982), Brovales syntectonic granite, Badajoz shear zone, Spain, and Berthé *et al.* (1979), syntectonic granites, South Armorican shear zone, France.

REFERENCES

Arthaud, F. 1969. Méthode de détermination graphique des directions de raccourcissement, d'allongement et intermédiaire d'une population de failles. *Bull. Soc. géol. Fr.*, 7 *Ser.* **111**, 729–737.

Bell, T. H. 1981. Foliation development—the contribution, geometry and significance of progressive, bulk, inhomogeneous shortening. *Tectonophysics* **75**, 273–296.

Berthé, D., Choukroune, P. & Jegouzo, P. 1979. Orthogneiss, mylonite and non-coaxial deformation of granites: the example of the South Armorican shear zone. *J. Struct. Geol.* **1**, 31–42.

Brun, J. P. & Pons, J. 1981. Strain patterns of pluton emplacement in a crust undergoing non-coaxial deformation, Sierra Morena, Southern Spain. *J. Struct. Geol.* **3**, 219–229.

Cobbold, P. R. 1977. Description and origin of banded deformation structures. I. Regional strain, local perturbations and deformation bands. *Can. J. Earth Sci.* **14**, 1721–1731.

Iglesias, M. & Choukroune, P. 1980. Shear zones in the Iberian Arc. *J. Struct. Geol.* **2**, 63–68.

Menard, G. 1980. Profondeur du socle antétriasique dans le sud-est de la France. *C. r. hebd. Séanc. Acad. Sci., Paris* **290**, 299–302.

Milnes, A. G. & Pfiffner, O. A. 1977. Structural development of the infrahelvetic complex, eastern Switzerland. *Eclog. geol. Helv.* **70**, 83–95.

Mitra, G. 1978. Ductile deformation zones and mylonites: the mechanical processes involved in the deformation of crystalline basement rocks. *Am. J. Sci.* **278**, 1057–1084.

Mitra, G. 1979. Ductile deformation zones in Blue Ridge Basement rocks and estimation of finite strains. *Bull. geol. Soc. Am.* **90**, 935–951.

Pons, J. 1982. Un modèle d'évolution de complexes plutoniques: Gabbros et granitoïdes de la Sierra Morena occidentale (Espagne). Thèse, Toulouse, France.

Ramsay, J. G. 1967. *Folding and Fracturing of Rocks*. McGraw-Hill, New York.

Ramsay, J. G. & Allison, J. 1979. Structural anlysis of shear zones in an Alpinised Hercynian granite. *Schweiz. Miner. Petrogr. Mitt.* **59**, 251–279.

Steck, A. 1966. Petrographische und tectonische Untersuchungen am Zentralen Aaregranit und seinen altkristallinen Hüllgesteinen im westlichen Aarmassiv. *Beitr. Geol. Karte Schweiz* (N.F.) **130**, 99.

Steck, A. 1968. Die alpidischen strukturen in den zentralen Aaregraniten des westlichen Aarmassivs. *Eclog. geol. Helv.* **61**, 19–48.

Steck, A., Ramsay, J. G., Milnes, A. G. & Burri, M. 1979. Compte-Rendu de l'excursion de la Société Géologique Suisse et la Société Suisse de Minéralogie et Pétrographie en Valais et en Italie du Nord du 2 au 5 octobre 1978. *Eclog. geol. Helv.* **72**, 287–311.

Voll, G. 1976. Recrystallisation of quartz, biotite and feldspars from Erstfeld to the Leventina Nappe, Swiss Alps and its geological significance. *Schweiz. Miner. Petrogr. Mitt.* **56**, 641–647.